

---

## ANALYSIS OF DYNAMICS OF TOPOLOGICAL PECULIARITIES OF VARYING RANDOM VECTOR LIGHT FIELDS

V.I. VASIL'EV, M.S. SOSKIN

UDC 535.4  
©2007

Institute of Physics, Nat. Acad. Sci. of Ukraine  
(46, Nauky Ave., Kyiv 03680, Ukraine; e-mail: vv@iop.kiev.ua)

---

The method of Stokes-polarimetry is applied to study the varying random optical fields. Mathematical methods, which allow  $C$ -points, saddle points, and bifurcation lines on the surface of an azimuth distribution and  $L$ -lines on the surface of a polarization handedness distribution to be determined, are proposed. The dynamics of a topological network at the development of photo-induced scattering in a  $\text{LiNbO}_3\text{:Fe}$  crystal has been analyzed. A reduction of the  $C$ -point density in time under the crystal irradiation has been revealed. The processes of creation and annihilation of the pairs of  $C$ -points have been analyzed.

### 1. Introduction

Singular optical fields reveal a number of interesting properties which attract the close attention of researchers for more than thirty years. To singular fields are classified those fields which contain points with uncertain parameters. In the case of scalar fields, only the phase can be indefinite. Around a point with uncertain phase, there emerges a phase helicoid (an optical vortex). In the case of elliptically polarized fields, there exist two parameters, which can be uncertain, namely, the tilt of the polarization ellipse with respect to the abscissa axis in the laboratory coordinate systems (the azimuth) and the direction of the electric vector rotation (the polarization handedness). If the azimuth is not determined, there appears a point with circular polarization (a  $C$ -point). The case of indefinite polarization handedness is associated with the geometrical place of points with a linear polarization (an  $L$ -line) [1].

One of the most interesting properties of singular fields is the circumstance that, in non-uniformly

elliptically polarized light fields (speckle-fields),  $C$ -points, saddle points on the surface of the distribution of polarization ellipse azimuths, and isoazimuthal lines crossing the saddle points (the bifurcation lines) form the so-called topological network [2]. The latter reflects the polarization structure of the field, and its study enables one to characterize both the speckle-field and the medium which generates the latter.

Challenging is the problem of studying the transformation of the topological network of a varying optical field. Earlier, it has been studied in the case of either singular beams propagating in a free space [3] or the controlled excitation of speckle-fields [4,5]. However, for practical implications, researches of the topological network response to the variations in the medium that generates a speckle-field would be more desirable. For example, it is required for the laser diagnostics of the shift or the deformation of a rough surface or for studying the processes in biosystems.

The study of the topological network of a varying light field is a rather complicated mathematical problem which demands a significant body of calculations. For instance, for studying the evolution of a topological network for only one realization of scattering, one has to determine the positions of and analyze the interrelations between about hundred thousand elements. It is impossible without creating special mathematical methods for processing the experimental data and realizing them in computer algorithms. In this work, we discuss the issues concerning the treatment of experimental data, which are presented in the form of a discrete set of the values of Stokes parameters, in detail.

The work aims at studying the evolution of the topological network which accompanies the development of photo-induced scattering in the LiNbO<sub>3</sub>:Fe crystal, by using the Stokes-polarimetry method. The phenomenon of photo-induced scattering occurs owing to the photorefractive recording of noise gratings, when the primary beam interacts with the light diffracted at micro-scale inhomogeneities of the crystal [6]. The scattering field is completely stochastic, being characterized by a speckle-structure. Since the photorefractive recording is not an instant process, the scattering develops slowly enough and becomes stationary within a time interval of tens of minutes. It allows the tiniest variations of the topological network to be studied and the stages of creation and annihilation of *C*-points to be carefully investigated.

## 2. General Consideration of the Problem

Consider a plane in the optical field cross-section which is perpendicular to the direction of field propagation. For the analysis of the field polarization state in such a cross-section, the Stokes parameters are the most frequently used ones. They are defined as follows:

$$\begin{cases} I_1 = I(0, 0), I_4 = I(135^\circ, 0), \\ I_2 = I(90^\circ, 0), I_5 = I(45^\circ, \frac{\pi}{2}), \\ I_3 = I(45^\circ, 0), I_6 = I(135^\circ, \frac{\pi}{2}), \end{cases} \begin{cases} S_0 = I_1 + I_2, \\ S_1 = I_1 - I_2, \\ S_2 = I_3 - I_4, \\ S_3 = I_5 - I_6, \end{cases} \quad (1)$$

where  $I(\varphi, \varepsilon)$  is the intensity of light that transmitted through a polarizer with azimuth  $\varphi$  and is characterizes by the delay  $\varepsilon$  of its vertical component with respect to the horizontal one.

For completely polarized light, the set of Stokes parameters is overdefined, so that an extra condition – in particular,  $S_0^2 = S_1^2 + S_2^2 + S_3^2$  – should be imposed. The parameters of the polarization ellipse and the Stokes parameters are connected by rather simple relations [7]. By analyzing the distributions of the Stokes parameters, one can determine the locations of *L*-lines, *C*-points, saddle points, and bifurcation lines.

The *L*-line is a border between sections with opposite polarization handednesses. The *C*-points are defined as the intersections of zero lines for  $S_1$  and  $S_2$ . In contrast to *L*-lines, *C*-points can be classified in several ways. First, it is the polarization handedness: there exist the right- and left-hand polarized *C*-points. Second, it is the value of the azimuth  $\Psi$  incursion at the path-tracing around a *C*-point. It is determined by the topological

index  $m$  as follows:

$$\oint_U d\Psi = 2\pi m, \quad (2)$$

where  $U$  is the contour that encircles the *C*-point. For random fields, the value of  $m$  can be equal to only  $\pm 1/2$ . The topological index can also be determined making use of the sign of the determinant [8]

$$D_I = S_{1x}S_{2y} - S_{1y}S_{2x}, \quad (3)$$

where  $S_{1x}$  and  $S_{1y}$  are the derivatives of  $S_1$  with respect to the spatial coordinates  $x$  and  $y$ , respectively; and  $S_{2x}$  and  $S_{2y}$  are the corresponding derivatives of  $S_2$ . If  $D_I > 0$ , the topological index  $m = -1/2$ ; if  $D_I < 0$ , then  $m = +1/2$ . Third, it is the type of ordering of polarization ellipses around the *C*-point. In stochastic vector fields, three forms can exist [1]. These forms differ from one another by the number and the positions of lines, at every point of which the large semi-axis of the ellipse is directed to the *C*-point (morphogenetic lines). The geometrical analysis showed that the sum of the path-tracing angle  $\theta$  and the azimuthal angle  $\Psi$  is equal to the expression

$$\Psi[r \cos(\theta), r \sin(\theta)] + \theta = k \frac{\pi}{2}, \quad (4)$$

where  $k = 1, 3$ , and  $5$  at any point of this line.

While trying the solution of the equation on a contour with variable radius  $r$  and with the center at the *C*-point, we obtain a sequence of points which determine the positions of morphogenetic lines. There may also exist the other possible approaches to the definition of such lines (work [9] and a private discussion with the participation of Prof. I. Freund). But all the approaches are equivalent and differ only from the viewpoint of the convenience of their application to computer-assisted processing.

The number of lines can be also determined with the help of the determinant [8]

$$\begin{aligned} D_L = & ((2S_{1y} + S_{2x})^2 - 3S_{2y}(2S_{1x} - S_{2y})) \times \\ & \times ((2tS_{1x} - S_{2y})^2 + 3S_{2x}(2S_{1y} - S_{2x})) - (2 \times \\ & \times S_{1x}S_{1y} + S_{1x}S_{2x} - S_{1y}S_{2y} + 4S_{2x}S_{2y})^2. \end{aligned} \quad (5)$$

If  $D_L < 0$ , there exist 3 lines, but only one in the case where  $D_L > 0$ . In general, three forms of *C*-points are possible: the topological index is equal to  $-1/2$ , and

there are three lines (a “star”); the topological index is equal to  $+1/2$ , and there is one line (a “lemon”); and the topological index is equal to  $+1/2$ , and there are three lines (a “monstar”) [1].

Hence, there are two approaches to the determination of the topological index of  $C$ -points and the morphology of a surrounding field: the integral approach [Eqs. (2) and (4)] and the differential one [Eqs. (3) and (5)]. Their equivalency can be demonstrated, but the integral approach is more interference-resistant from the viewpoint of the processing of experimental data. It is also worth noting that Eq. (4), in contrast to Eq. (5), determines not only the number of lines but also their positions.

In order to determine the positions of saddle points on the surface of an azimuthal distribution, it is necessary to find points, where the conditions

$$\Psi_x = 0, \Psi_y = 0, \Psi_{xx} \cdot \Psi_{yy} - \Psi_{xy}^2 < 0 \quad (6)$$

are satisfied.

If an isoazimuthal line passes through a saddle point, we obtain the so-called bifurcation line. The bifurcation line can either finish at  $C$ -points (a “dipole” and a “quadrupole”) or be closed (an “eight”) [3].

All the elements of the topological grid of an elliptic field satisfy the Poincaré–Hopf conservation law of the total topological index ( $-1$  for every saddle point, and  $\pm 1/2$  for every  $C$ -point) and the rule of signs [3]. Topological reactions are possible only between  $C$ -points with the same polarization and the opposite topological indices. These rules must be obeyed even if the perturbations of the optical field are strong.

### 3. Experimental Part

The experimental setup is exhibited in Fig. 1. Radiation emission with a wavelength of  $0.63 \mu\text{m}$  generated by a helium-neon laser  $1$  was narrowed to a diameter of  $0.5 \text{ mm}$  with the help of telescope  $2$  and passed through  $\text{LiNbO}_3\text{:Fe}$  crystal  $5$  doped with iron to  $0.05 \text{ wt.}\%$ . The inclination of the beam polarization plane was controlled with the use of half-wave plate  $3$ . First, the crystal was irradiated in such a manner that the polarization vector was perpendicular to the main axis  $c$  of the crystal  $I$ . In this case, an ordinary wave propagated in the medium. The scattering field was linearly polarized, and the polarization azimuth coincided with the azimuth of the initial beam. In 35 min, the process of scattering became stationary. Then, half-wave plate  $3$  was turned in such a manner that the angle between the polarization

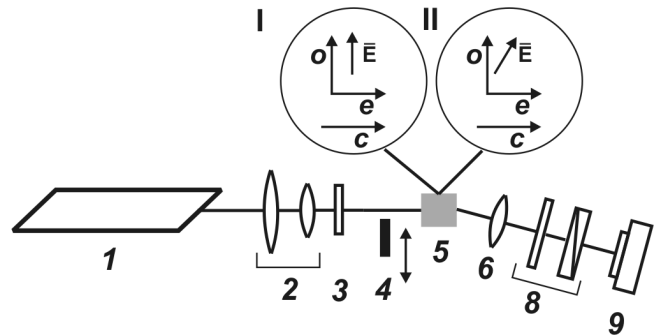


Fig. 1. Scheme of experimental setup

vector of the laser beam and the axis  $c$  became equal to  $59^\circ$   $II$ , so that the difference between diffraction efficiencies for the ordinary and extraordinary waves became compensated. In such a geometry of recording and reading the noise gratings, the scattering field was elliptically polarized and had no prevailing component. The component, which corresponded to the extraordinary wave, started to record noise gratings, which competed with those recorded earlier. The process of scattering ceased to be stationary, and the speckle field began to smear. Both the intensity distribution and its polarization structure changed completely and stochastically. The scattered radiation was collimated making use of lens  $6$  and was analyzed with the help of Stokes-analyzer  $8$  and a CCD-chamber. The Stokes-analyzer consisted of a quarter-wave plate (the error was about  $\lambda/100$ ) and a polarizer with a polarization ability of  $1/500$ . The relative error of the determination of the intensity of Stokes-parameters was induced by the imperfection of optical elements and was equal to  $4\%$ . Scattering at an angle of  $6^\circ$  (the analyzed section was  $1.5 \times 10^4 \text{ sr}$ ) was analyzed.

Since intensities (1) are measured within a finite time interval at the determination of Stokes parameters, a certain restriction has to be imposed on the rate of variation of the field concerned. The restriction can be expressed as follows:

$$\frac{I_i(\tau) - I_i(0)}{I_i(T) - I_i(0)} \ll 1, \quad i = 1, 2, \dots, 6, \quad (7)$$

where  $T$  is the time interval between consecutive measurements, and  $\tau$  is the measurement time of all Stokes parameters. To satisfy condition (7), the beam was cut off with the help of electromechanical latch  $4$  in the course of the realignment of a polarizer and a quarter-wave-plate. In  $\text{LiNbO}_3\text{:Fe}$ , the characteristic time-scale of the processes that run in dark comprises

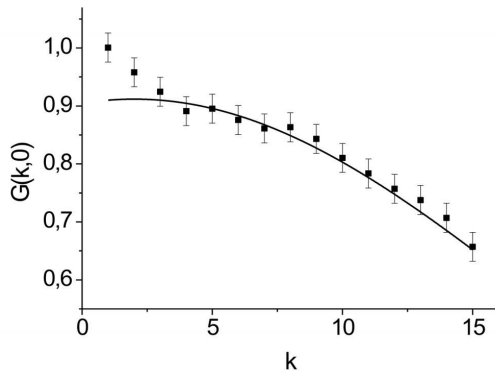


Fig. 2. Correlation  $G(k, 0)$  between the first and the  $k$ -th pattern at the development of photo-induced scattering. The time interval between making frames was 5 s. The magnitude of the additive noise dispersion was evaluated to be 0.091

several months. Therefore, we may assume that the state of noise gratings does not change in the absence of their illumination. The crystal was irradiated for 15 s between the measurements of a polarization state; the total exposition time during a measurement was 0.6 s. The largest error of quantity (7) was 3%.

Owing to the presence of noises in the pattern, a straightforward mathematical processing of intensity distributions in a CCD-chamber is impossible. The sources of noise are both the redistribution of charges in the semiconducting matrix and the pattern discretization, as well as the electromagnetic disturbances emerging at the transmission of a signal from the chamber to a computer. For the filtration of such noises to be correct, the most frequently used filtration procedure is the adaptive Wiener one [10]. For the Wiener algorithm to be applied, it is necessary to determine the statistical parameters of noise. This can be done by calculating the correlation  $G(k, 0)$  between the first and the  $k$ -th pattern in the sequence of frames describing the development of photo-induced scattering [11]. The function  $G(k, 0)$  for photo-induced scattering varies slowly at small  $k < 3$  (the characteristic time is about 35 min). If the pattern includes noise – which, as a rule, does not correlate with the pattern and the characteristic time is measured in seconds – the function  $G(k, 0)$  drastically increases at small  $k$  [12]. Having extrapolated the dependence  $G(k, 0)$  for the patterns with large  $k > 3$  into the range of small  $k$ , one may accept the difference between the extrapolated and the measured correlation as an estimation of the dispersion of an additive non-correlated noise [11]. Figure 2 demonstrates a typical dependence  $G(k, 0)$  for the development of scattering.

To verify the correctness of filtration, we made a reference experiment with a stationary diffuser (depolished glass). Fifty frames of a still speckle field separated by a 5-s time interval were photographed. The average distribution of intensity in this sequence was accepted as a true distribution. The noise-to-signal ratio was 8.9%. After treating the patterns with the help of a Wiener filter, the noise-to-signal ratio became reduced to the value of 1.6%. The total relative measurement error for the values of Stokes parameters was equal to 5.2%.

In order to determine the position of each element of the topological network, it is necessary to pass from the analysis of continuous functions, which are used to construct the theory, to the analysis of discrete distributions of Stokes parameters. In a pixel coordinate system  $(i, j)$ , the  $L$ -line is defined as the geometrical place of points, for which the condition

$$(S_3(i, j) \cdot S_3(i + 1, j) < 0) \vee (S_3(i, j) \cdot S_3(i, j + 1) < 0) \vee (S_3(i, j + 1) \cdot S_3(i + 1, j + 1) < 0) = 1$$

is satisfied. The  $C$ -point is defined as a point, for which the condition

$$(S_1(i, j) \cdot S_1(i + 1, j) < 0 \vee S_1(i, j) \cdot S_1(i, j + 1) < 0 \vee S_1(i, j + 1) \cdot S_1(i + 1, j + 1) < 0) \wedge (S_2(i, j) \times S_2(i + 1, j) < 0 \vee S_2(i, j) \cdot S_2(i, j + 1) < 0 \vee S_2(i, j + 1) \cdot S_2(i + 1, j + 1) < 0) = 1$$

is satisfied. The topological index of a  $C$ -point and the number of morphogenetic lines are determined by the sign of the finite-difference approximation of the determinants  $D_I$  and  $D_L$ :

$$D_I = (S_1(i + 1, j) - S_1(i, j)) \cdot (S_2(i, j + 1) - S_2(i, j)) - (S_1(i, j + 1) - S_1(i, j)) \cdot (S_2(i + 1, j) - S_2(i, j));$$

$$D_L = ((2(S_1(i, j + 1) - S_1(i, j)) + (S_2(i + 1, j) - S_2(i, j)))^2 - 3(S_2(i, j + 1) - S_2(i, j)) \times (2(S_1(i + 1, j) - S_1(i, j)) - (S_2(i, j + 1) - S_2(i, j))))$$

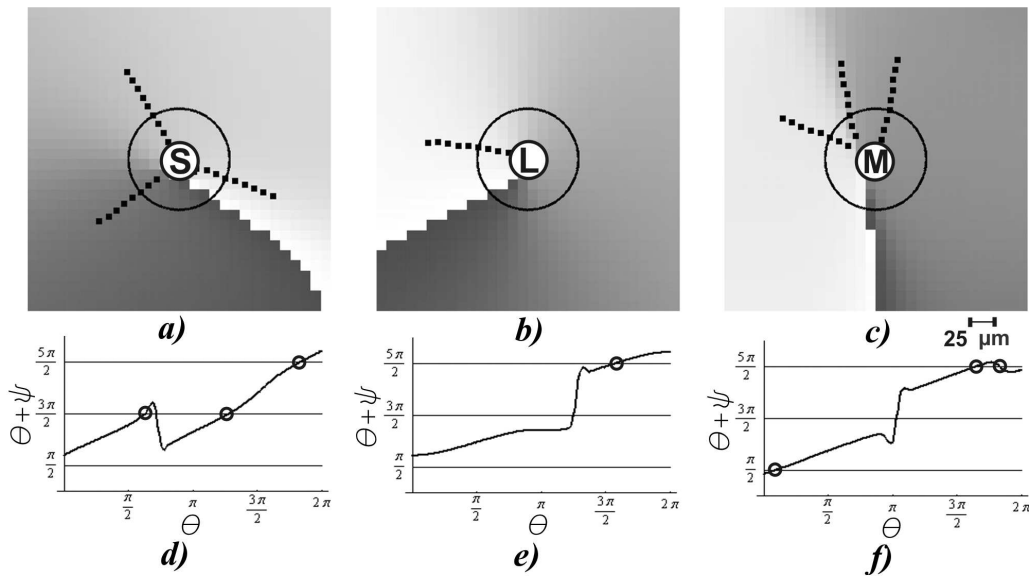


Fig. 3. Positions of morphogenetic lines around the  $C$ -points of the “star” (a), “lemon” (b), and “monstar” (c) types. The corresponding dependences of the sum  $(\Psi + \theta)$  of the azimuthal and path-tracing angles on the path-tracing angle  $\theta$  for path-tracing along a circle  $40 \mu\text{m}$  in radius (d–f)

$$\begin{aligned}
 & -S_2(i, j))) \cdot ((2(S_1(i + 1, j) - S_1(i, j)) - \\
 & -(S_2(i, j + 1) - S_2(i, j)))^2 + 3(S_2(i + 1, j) - \\
 & -S_2(i, j) \cdot (2(S_1(i, j + 1) - S_1(i, j)) - (S_2(i + 1, j) - \\
 & -S_2(i, j))) - (2(S_1(i + 1, j) - S_1(i, j)) \cdot (S_1(i, j + 1) - \\
 & -S_1(i, j)) + (S_1(i + 1, j) - S_1(i, j)) \cdot (S_2(i + 1, j) - \\
 & -S_2(i, j)) - (S_1(i, j + 1) - S_1(i, j)) \cdot (S_2(i, j + 1) - \\
 & -S_2(i, j)) + 4(S_2(i + 1, j) - S_2(i, j) \cdot (S_2(i, j + 1) - \\
 & -S_2(i, j)))^2.
 \end{aligned}$$

The morphogenetic line was found as a set of points, for which expression (4) is satisfied. In Fig. 3, the experimentally obtained distribution of the morphogenetic lines around a  $C$ -point is depicted.

We note that the solution of Eq. (4) which corresponds to a discontinuity of the azimuth distribution at the edges of the  $[0, \pi]$ -interval (on the plot, they look like sharp jumps, but are not the points of morphogenetic lines) is not analyzed in this work.

The saddle points are defined using the discrete representation of condition (6):

$$(\Psi(i + 1, j) - \Psi(i, j) \cdot (\Psi(i, j) - \Psi(i - 1, j) < 0) \vee$$

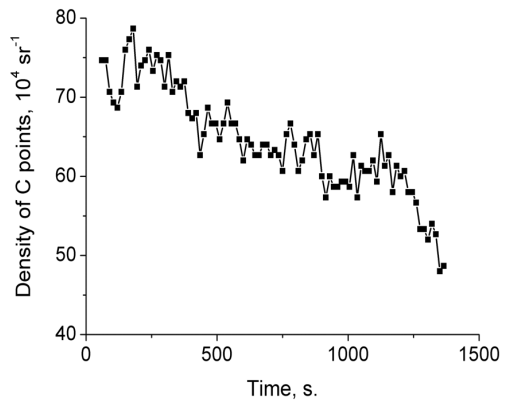


Fig. 4. Evolution of the  $C$ -point density at scattering development

$$\vee (\Psi(i, j + 1) - \Psi(i, j) \cdot (\Psi(i, j) - \Psi(i, j - 1) < 0) \vee$$

$$\vee (((\Psi(i - 1, j) - 2\Psi(i, j) + \Psi(i + 1, j)) \cdot (\Psi(i, j - 1) -$$

$$-2\Psi(i, j) + \Psi(i, j + 1)) - (\Psi(i + 1, j + 1) -$$

$$-\Psi(i, j + 1) - \Psi(i + 1, j) + \Psi(i, j))^2) < 0) = 1.$$

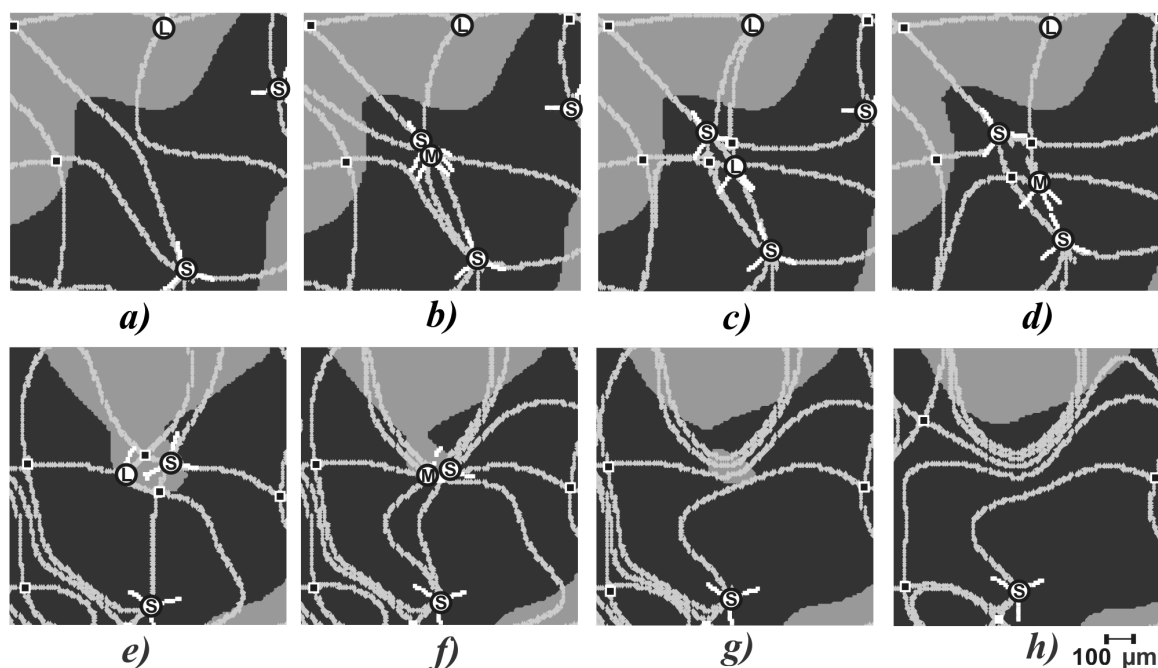


Fig. 5. Creation (*a–d*) and annihilation (*e–h*) of *C*-point pairs. The time interval between the frames of corresponding series is 15 s. Grey and black colors correspond to left- and right-hand polarization, respectively. Circles with letters denote the type of *C*-points: S stands for “star”, *L* for “lemon”, and *M* for “monstar”. Grey lines correspond to bifurcation lines. White lines near *C*-points correspond to the orientations of morphogenetic lines. Black squares correspond to the positions of saddle points

The bifurcation lines are determined from the condition

$$(\Psi_p^i(i, j) \cdot \Psi_p^i(i + 1, j) < 0) \vee (\Psi_p^i(i, j) \cdot \Psi_p^i(i, j + 1) < 0) \vee (\Psi_p^i(i, j + 1) \cdot \Psi_p^i(i + 1, j + 1) < 0) = 1,$$

where  $\Psi_p^i = \Psi - \Psi_s^i$ , and  $\Psi_s^i$  is the azimuth of the *i*-th saddle point. Such an algorithm of searching the bifurcation lines produces fault solutions in the form of lines at discontinuities of the azimuth distribution. To verify the solution, we artificially rotated the coordinate system. In contrast to the azimuth distribution discontinuities, the positions of bifurcation lines and *C*-points are invariant with respect to the coordinate-rotation transformation.

On the basis of these mathematical methods, we create a computer program which automatically determines the positions of *L*-lines, the number, the positions, and the types of *C*-points, and the positions of morphological lines; it also visualized the topological network. By using this program, we get the experimental data analyzed in what follows.

#### 4. Results and Their Discussion

A typical dependence of the density of *C*-points on the illumination time in the studied field region is depicted in Fig. 4. The density of singularities in the scattering field may testify to certain characteristic scales of the scattering medium. In work [13], this was shown for the photorefractive interaction between two waves in a Bi<sub>12</sub>SiO<sub>12</sub> crystal, where the density of optical vortices depended on the Fresnel number of either wave.

There is a physical analogy between optical vortices for scalar fields and *C*-points for vector ones. With a large reliability, one may assume that the reduction of the *C*-point density can be a consequence of the reduction of the number of interfering waves, which evidences, in turn, for an increase of the characteristic dimensions of photo-induced inhomogeneities.

The reduction of the *C*-point density is possible only if the number of annihilations exceeds the number of creations. As was already said, a creation or an annihilation event is possible only between the *C*-points with the same polarization and different topological indices. As a consequence of the sign rule [3], every event of creation or annihilation

stimulates a modification of the topological network in general. In Fig. 5, the typical scenarios of the creation and annihilation of the pairs of  $C$ -points are exhibited. It is always the pairs “star”–“monstar” that are created or annihilate (Figs. 5,  $a$ – $b$  and  $e$ – $f$ ) with a preliminary transformation “lemon” $\leftrightarrow$ “monstar”. Figures 5,  $e$ – $h$  illustrate the fact that the field region, which contains  $C$ -points, cannot change its polarization handedness without a preliminary annihilation of all  $C$ -points.

## 5. Conclusions

In this work, we have proposed methods for the determination of the positions and characteristics of  $C$ -points,  $L$ -lines, and saddle points on the surface of a distribution of polarization ellipse azimuths, as well as bifurcation lines. With their help, we have studied the evolution of the topological network of the photo-induced scattering field in the course of its development. A reduction of the density of  $C$ -points during the scattering development has been demonstrated, which can be associated with the growth of the characteristic dimensions of photo-induced inhomogeneities. For the first time, the processes of creation and annihilation under the condition of random perturbations of the optical field were studied. The transformation of the topological network was demonstrated to obey the rules found for the propagation in a free space and a controlled perturbation.

The authors are grateful to the Corresponding member of the National Academy of Sciences of Ukraine Prof. S.G. Odoulov and Ph.D. A.N. Shumelyuk for supplying them with  $\text{LiNbO}_3\text{:Fe}$  crystals and for the fruitful proposals.

1. J.F. Nye, *Natural Focusing and Fine Structure of Light: Caustics and Wave Dislocations* (Institute of Physics Publ. House, Bristol, 1999).

2. M. Soskin, V. Denisenko, and R. Egorov, *J. Opt. A: Pure Appl. Opt.* **6**, 281 (2004).
3. I. Freund, M.S. Soskin, and A. Mokhun, *Opt. Commun.* **208**, 223 (2002).
4. I. Freund, *Opt. Lett.* **29**, 15 (2004).
5. R.I. Egorov, V.G. Denisenko, and S.M. Soskin, *JETP Lett.* **81**, 464 (2005).
6. *Photorefractive Crystals and Applications*, edited by J.-P. Huignard and P. Guenter (Springer, Heidelberg, 1989).
7. M. Born and E.W. Wolf, *Principles of Optics* (Pergamon Press, Oxford, 1991).
8. M.R. Dennis, *Opt. Commun.* **231**, 201 (2002).
9. R.I. Egorov, Ph.D. thesis (Kyiv, 2007).
10. L. Rabiner and B. Gould, *Theory and Application of Digital Signal Processing* (Prentice-Hall, Englewood Cliffs, 1975).
11. L.P. Yaroslavskii, *Introduction to Digital Image Processing* (Sovetskoe Radio, Moscow, 1979) (in Russian).
12. L.I. Mirkin, *Vopr. Kibernet.: Ikonika, Tsyfr. Obrab. Filtr. Izobr.* **38**, 73 (1978).
13. F.T. Arecchi, G. Giacomelli *et al.*, *Phys. Rev. Lett.* **67**, 3749 (1991).

Received 31.07.07.

Translated from Ukrainian by O.I. Voitenko

АНАЛІЗ ДИНАМІКИ ТОПОЛОГІЧНИХ ОСОБЛИВОСТЕЙ  
ВИПАДКОВИХ ВЕКТОРНИХ СВІТЛОВИХ ПОЛІВ,  
ЩО ЗМІНЮЮТЬСЯ

*В.І. Васильєв, М.С. Соскін*

Резюме

Розглянуто стокс-поляриметрию випадкових оптичних полів, що змінюються. Запропоновано математичні методи пошуку  $C$ -точок, сідлових точок, біфуркаційних ліній на поверхні азимутального розподілу та  $L$ -ліній на поверхні розподілу знака поляризації. Ці методи застосовано до експериментального дослідження неоднорідно еліптично поляризованих світлових полів. Досліджено динаміку топологічної сітки під час розвитку фотоіндукованого розсіяння у кристалі  $\text{LiNbO}_3\text{:Fe}$ . Виявлено зменшення щільності  $C$ -точок зі збільшенням часу опромінення. Проаналізовано процеси народження та анігіляції пар  $C$ -точок.